





# Unstable Convection in a Vertical Double–Layer Porous Slab

Stefano Lazzari <sup>1,\*</sup>, Michele Celli <sup>2,†</sup>, Antonio Barletta <sup>2,†</sup> and Pedro Vayssière Brandão <sup>2,†</sup><sup>1</sup> Department of Architecture and Design, University of Genoa, Stradone S. Agostino 37, 16123 Genoa, Italy<sup>2</sup> Department of Industrial Engineering, Alma Mater Studiorum Università di Bologna, Viale Risorgimento 2, 40136 Bologna, Italy; michele.celli3@unibo.it (M.C.); antonio.barletta@unibo.it (A.B.); pedro.vayssiere2@unibo.it (P.V.B.)

\* Correspondence: stefano.lazzari@unige.it

† These authors contributed equally to this work.

**Abstract:** A convective stability analysis of the flow in a vertical fluid-saturated porous slab made of two layers with different thermophysical properties is presented. The external boundaries are isothermal with one of them impermeable while the other is open to an external fluid reservoir. This study is a development of previous investigations on the onset of thermal instability in a vertical heterogeneous porous slab where the heterogeneity may be either continuous or piecewise as determined by a multilayer structure. The aim of this paper is investigating whether a two-layer structure of the porous slab may lead to the onset of cellular convection patterns. The linear stability analysis is carried out under the assumption that one porous layer has a thermal conductivity much higher than the other layer. This assumption may be justified for the model of a heat transfer enhancement system involving a saturated metal foam. A flow model for the natural convection based on Darcy’s momentum transfer in a porous medium is adopted. The buoyancy-induced basic flow state is evaluated analytically. Small-amplitude two-dimensional perturbations of the basic state are introduced, thus leading to a linear set of governing equations for the disturbances. A normal mode analysis allows one to formulate the stability eigenvalue problem. The numerical solution of the stability eigenvalue problem provides the onset conditions for the thermal instability. Moreover, the results evidence that the permeability ratio of the two layers is a key parameter for the critical conditions of the instability.



**Citation:** Lazzari, S.; Celli, M.; Barletta, A.; Brandão, P.V. Unstable Convection in a Vertical Double–Layer Porous Slab. *Energies* **2023**, *16*, 4938. <https://doi.org/10.3390/en16134938>

Academic Editor: Jose A. Almendros-Ibanez

Received: 10 May 2023

Revised: 8 June 2023

Accepted: 15 June 2023

Published: 25 June 2023



**Copyright:** © 2023 by the authors. Licensee MDPI, Basel, Switzerland. This article is an open access article distributed under the terms and conditions of the Creative Commons Attribution (CC BY) license (<https://creativecommons.org/licenses/by/4.0/>).

**Keywords:** multilayer porous slab; linear stability; convection; buoyant flow; metal foam

## 1. Introduction

Studies on the stability of natural convection flow in a vertical porous slab have been carried out for decades due to their important implications in a wide range of energy applications, ranging from thermal insulation of buildings to low-enthalpy geothermal systems, from filtration processes to heat transfer enhancement systems. In 1969, Gill [1] proved that in a vertical porous slab confined by two impermeable boundaries kept at different yet uniform temperatures, a conduction regime can be maintained, without any instability for all values of the Darcy–Rayleigh number. This result has been found rigorous by considering the slab saturated by a Newtonian fluid and by adopting Darcy’s law and the Boussinesq approximation. Gill [1] pointed out “the viscous–fluid analogue of the problem studied in this paper is of interest in connection with building insulation involving an unventilated air gap. . . . Then a cellular motion occurs which will increase the heat transfer considerably”. Thus, the stability results for the porous slab reveal that the use of a porous insulation material filling the air gap prevents the emergence of convection heat transfer.

Several authors have extended Gill’s study by considering features such as the nonlinearity of the perturbation dynamics, momentum transfer models for the seepage flow in the porous medium providing extensions of Darcy’s law and local thermal non-equilibrium

models for the local energy balance [2–7]. On the other hand, some authors have investigated different boundary conditions for the vertical slab and found that instabilities may arise when the boundaries are permeable [8–12].

A study carried out by Barletta [8] reconsidered the thermoconvective stability problem in a porous vertical slab formulated by Gill [1] under the assumption of isothermal, but permeable, boundaries. Even though the change in the velocity boundary conditions does not affect the basic natural convection flow, which remains the same stationary and parallel flow obtained by Gill [1], it does drastically affect the stability analysis. Indeed, the flow in the basic state becomes unstable when the Darcy–Rayleigh number is larger than 197.081 and the normal modes selected at onset of instability are transverse rolls.

Multilayered porous media, a fascinating and versatile technology, has gained significant attention in various industries and fields due to its wide range of applications. These heterogeneous materials consist of multiple layers with interconnected pores, offering enhanced functionalities and improved performance compared to traditional single-layered porous media. By leveraging their distinct properties, multilayered porous media open up interesting possibilities for advancements in fields such as oil and gas, environmental remediation, water filtration, biomedical and pharmaceutical, chemical and petrochemical, construction and civil engineering, and aerospace and automotive industries. The application of multilayered porous media is promising in numerous areas. It offers enhanced filtration efficiency, allowing for better separation and purification of substances in industries such as water treatment, oil and gas reservoir engineering, and membrane filtration systems. The ability to control fluid flow offers opportunities for improving heat exchangers, thermal management systems, and even acoustic and vibration dampening applications. The retention of contaminants and enhanced structural stability make it valuable in environmental remediation efforts and construction projects where filtration and long-term durability are crucial.

However, the practical implementation of multilayered porous media does come with certain challenges. Manufacturing complexity, cost considerations, difficulties in customization, and uncertainty in long-term performance are factors that need to be addressed for widespread adoption. Furthermore, the lack of standardized testing methods and limited understanding of design parameters pose additional hurdles. Nonetheless, ongoing research and advancements in this field continue to address these challenges and propel the development of multilayered porous media towards real-world applications.

The motivation of the research on convection in multilayered structures of a porous slab saturated by a fluid relies on the possibility to improve the design criteria for the optimization of the heat transfer devices. In fact, the study of the conditions for the onset of convective cellular patterns in a vertical porous slab offers novel and important knowledge for the development of design strategies oriented to the heat transfer enhancement and the thermal energy storage [13]. Furthermore, the thermal behaviour of fluids or phase change materials (PCM) saturating metallic or ceramic foams allows a significant advancement by providing robust design rules for compact thermal storage systems and compact heat exchangers. Another target is the engineering of buildings and, in particular, the use of breathing walls [14].

In a recent paper [15], the study by Gill [1] has been further extended to a sandwiched vertical porous slab with impermeable isothermal boundaries kept at different temperatures. In detail, the authors assumed a slab made of three porous layers saturated by a Newtonian fluid, where the two external layers are identical and with a thermal conductivity much higher than that of the central layer. For this symmetric configuration, it is found that the basic buoyant flow in the internal core is identical to that devised by Gill [1], namely, that it is characterized by a stationary and purely vertical velocity field. On the other hand, when this basic state is perturbed, the two interfaces with the external layers may allow for a horizontal flow contribution. It is worth noting that, when the focus is on the core layer, the sandwiched slab represents a relaxation in the original Gill problem, the impermeable boundaries being substituted by two permeable interfaces with the external layers. The

three-layer slab is, in fact, a horizontally heterogeneous medium with a piecewise constant permeability, in analogy with the continuously heterogeneous slab studied by Shankar and Shivakumara [16]. Barletta et al. [15] pointed out that a sufficiently large Darcy–Rayleigh number can lead to flow instability and that the neutral stability condition depends on the permeability ratio between the external layers and the core layer, as well as on the ratio between the overall thickness of the slab and that of the core layer. Moreover, for the limiting case where the permeability ratio tends to infinity, the condition for the onset of the instability coincides with that predicted by Barletta [8] for a homogeneous porous layer with permeable boundaries.

In order to further develop the findings presented by Barletta et al. [15], other multilayer configurations can be explored. In the present paper, a two-layer vertical porous slab will be investigated, under the assumptions that the layers have the same width and that one layer is a metal foam, i.e., it has an extremely high thermal conductivity. As in the original problem faced by Gill [1], the boundaries of the slab are isothermal with different temperatures. However, we will consider conditions where one boundary is permeable while the other is impermeable. The basic state flow will be determined and a linear stability analysis will be performed by assuming small-amplitude wavelike disturbances. The threshold values of the Darcy–Rayleigh number for the onset of the instability will be evaluated numerically. It will be shown that the transverse rolls are the most unstable. The asymmetry in the geometrical and physical configuration leads to transverse rolls that are non-stationary, but travelling. Moreover, the limiting cases where the ratio between the permeability of the two layers vanishes or tends to infinity will be investigated.

## 2. Mathematical Model

An infinitely high vertical slab composed by two different porous layers having the same width  $L$  is considered, as illustrated in Figure 1. The slab is saturated by a Newtonian fluid and it is characterized by an open and isothermal boundary at  $x = 0$  and an impermeable and isothermal boundary at  $x = 2L$ . The open boundary at  $x = 0$  is modeled by imposing a purely hydrostatic pressure distribution.

The mass, momentum and energy local balance equations together with the boundary conditions employed can be written as

$$\begin{aligned} \nabla \cdot \mathbf{u}_i &= 0, \\ \frac{\mu}{K_i} \mathbf{u}_i &= -\nabla P_i + \rho_0 g \beta (T_i - T_0) \hat{\mathbf{e}}_z, \\ \sigma_i \frac{\partial T_i}{\partial t} + \mathbf{u}_i \cdot \nabla T_i &= \alpha_i \nabla^2 T_i, \\ x = 0 : \quad P_1 &= 0, \quad T_1 = T_l, \\ x = 2L : \quad \frac{\partial P_2}{\partial x} &= 0, \quad T_2 = T_r, \end{aligned} \quad (1)$$

where the index  $i = 1, 2$  distinguishes between layer 1 and layer 2. In Equation (1),  $\mathbf{u} = (u, v, w)$  is the velocity,  $T$  is the temperature,  $P$  is the local difference between the pressure and the hydrostatic pressure (hereafter, it will be called simply pressure for the sake of brevity),  $t$  is the time,  $\mu$  is the dynamic viscosity,  $K$  is the permeability,  $\rho_0$  is the fluid density evaluated at the reference temperature  $T_0$ ,  $g$  is the modulus of the gravitational acceleration  $g$ ,  $\hat{\mathbf{e}}_z$  is the unit vector along the  $z$  axis,  $\beta$  is the thermal expansion coefficient,  $\sigma$  is the heat capacity ratio of the saturated porous medium,  $\alpha$  is the effective thermal diffusivity of the saturated porous medium (the weighted arithmetic mean of the solid and fluid thermal conductivities divided by the fluid heat capacity per unit volume) and  $T_l$  is the temperature of the left hand boundary while  $T_r$  is the temperature of the right hand boundary. In Equation (1), Darcy's law is adopted together with the Oberbeck–Boussinesq approximation. The impermeability condition at  $x = 2L$  has been expressed in terms

of pressure by employing Darcy’s law since, in the following, a pressure–temperature formulation is used.

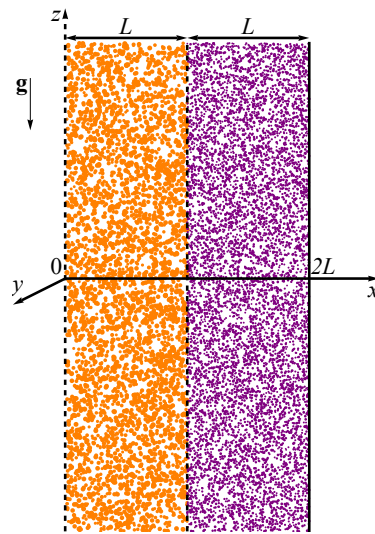


**Figure 1.** Cross-section of the porous slab on a plane  $y = \text{constant}$ . The orange fill color denotes layer 1, while the violet fill color denotes layer 2.

Accordingly, the interface conditions that define the continuity of the pressure, of the velocity component  $u$ , of the temperature and of the heat flux density in the  $x$ -direction, have the form

$$x = L : \quad P_1 = P_2, \quad K_1 \frac{\partial P_1}{\partial x} = K_2 \frac{\partial P_2}{\partial x}, \quad T_1 = T_2, \quad \alpha_1 \frac{\partial T_1}{\partial x} = \alpha_2 \frac{\partial T_2}{\partial x}. \quad (2)$$

It is worth noting that the ratio  $\alpha_2/\alpha_1$  coincides with the ratio between the thermal conductivities of the two porous layers since the fluid saturating both layers is the same.

*Pressure–Temperature Formulation*

The dimensionless problem is formulated differently for the two layers. The dimensionless governing equations for layer 1 are

$$\begin{aligned} \nabla^2 P_1 &= R \frac{\partial T_1}{\partial z}, \\ \frac{\partial T_1}{\partial t} - \nabla P_1 \cdot \nabla T_1 + R T_1 \frac{\partial T_1}{\partial z} &= \nabla^2 T_1, \end{aligned} \quad (3)$$

and, for layer 2,

$$\begin{aligned} \nabla^2 P_2 &= R \frac{\partial T_2}{\partial z}, \\ \tau \frac{\partial T_2}{\partial t} - \xi \nabla P_2 \cdot \nabla T_2 + R \xi T_2 \frac{\partial T_2}{\partial z} &= \gamma \nabla^2 T_2, \end{aligned} \quad (4)$$

while the boundary and interface conditions are

$$\begin{aligned} x = 0 : \quad & P_1 = 0, \quad T_1 = \eta, \\ x = 1 : \quad & P_1 = P_2, \quad \frac{\partial P_1}{\partial x} = \xi \frac{\partial P_2}{\partial x}, \quad T_1 = T_2, \quad \frac{\partial T_1}{\partial x} = \gamma \frac{\partial T_2}{\partial x}, \\ x = 2 : \quad & \frac{\partial P_2}{\partial x} = 0, \quad T_2 = 1 + \eta. \end{aligned} \quad (5)$$

where  $\eta = (T_l - T_0)/\Delta T$ , with  $\Delta T = T_r - T_l$ . In Equations (3)–(5), the scaling

$$\frac{t}{\sigma_1 L^2 / \alpha_1} \rightarrow t, \quad \frac{(x, y, z)}{L} \rightarrow (x, y, z), \quad \frac{\mathbf{u}_i}{\alpha_1 / L} \rightarrow \mathbf{u}_i, \quad \frac{P_i}{\mu \alpha_1 / K_1} \rightarrow P_i, \quad \frac{T_i - T_0}{\Delta T} \rightarrow T_i, \quad (6)$$

is employed, together with the dimensionless parameters

$$R = \frac{\rho_0 g \beta \Delta T K_1 L}{\mu \alpha_1}, \quad \xi = \frac{K_2}{K_1}, \quad \gamma = \frac{\alpha_2}{\alpha_1} \quad \tau = \frac{\sigma_2}{\sigma_1}, \quad (7)$$

where  $R$  is the Darcy–Rayleigh number.

### 3. Basic State

The basic stationary solution of the system given by Equations (3)–(5), whose stability has to be investigated, is assumed to be a fully developed buoyant flow in the vertical  $z$ -direction with zero net mass flow rate, namely

$$P_{1b} = 0 = P_{2b}, \quad T_{1b} = -\frac{3\gamma - 4\gamma x + 1}{4(\gamma + 1)}, \quad T_{2b} = \frac{\gamma + 4x - 5}{4(\gamma + 1)},$$

$$\mathbf{u}_{1b} = (0, 0, R T_{1b}), \quad \mathbf{u}_{2b} = (0, 0, R \xi T_{2b}), \quad (8)$$

where the subscript  $b$  denotes the quantities relative to this basic state. Because of the interface conditions, the temperature distribution inside the slab is a piecewise linear function of  $x$ , as reported in Figure 2 for given values of  $\gamma$ . Equation (8) is obtained by defining the reference temperature  $T_0$  as the average temperature of the slab, so that

$$\int_0^2 T_b \, dx = 0. \quad (9)$$

The choice expressed by Equation (9) yields

$$\eta = -\frac{3\gamma + 1}{4(\gamma + 1)}. \quad (10)$$

Both the limiting cases of  $\gamma \rightarrow 0$  and  $\gamma \rightarrow \infty$  yield a vanishing temperature gradient in one of the two layers. From Equation (8) one can notice that the velocity has a discontinuity at the interface except for the case  $\xi = 1$ .

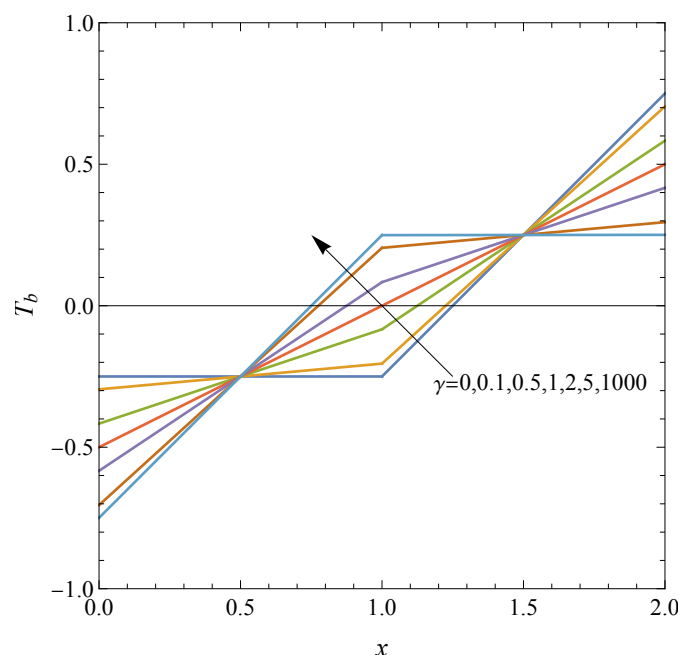


Figure 2. Plots of  $T_b$  versus  $x$  for fixed values of  $\gamma$ .

#### 4. The Limiting Case of a Highly Conductive Porous Layer

Let us assume that the thermal conductivity of the porous layer 2 is much greater than the thermal conductivity of the porous layer 1. This assumption yields the limiting case  $\gamma \rightarrow \infty$ , which can be devised by considering layer 2 as a metal foam, for instance. For this limiting case, the basic state given by Equation (8) reduces to

$$P_{1b} = 0 = P_{2b}, \quad T_{1b} = x - \frac{3}{4}, \quad T_{2b} = \frac{1}{4}, \quad \mathbf{u}_{1b} = (0, 0, R T_{1b}), \quad \mathbf{u}_{2b} = (0, 0, R \zeta T_{2b}), \quad (11)$$

while the governing Equations (3)–(5) simplify to

$$\begin{aligned} \nabla^2 P_1 &= R \frac{\partial T_1}{\partial z}, \quad \frac{\partial T_1}{\partial t} - \nabla P_1 \cdot \nabla T_1 + R T_1 \frac{\partial T_1}{\partial z} = \nabla^2 T_1, \\ \nabla^2 P_2 &= R \frac{\partial T_2}{\partial z}, \quad \nabla^2 T_2 = 0, \\ x = 0 : \quad P_1 &= 0, \quad T_1 = -\frac{3}{4}, \\ x = 1 : \quad P_1 &= P_2, \quad \frac{\partial P_1}{\partial x} = \zeta \frac{\partial P_2}{\partial x}, \quad T_1 = T_2, \quad \frac{\partial T_2}{\partial x} = 0, \\ x = 2 : \quad \frac{\partial P_2}{\partial x} &= 0, \quad T_2 = \frac{1}{4}. \end{aligned} \quad (12)$$

#### 5. Linear Stability Analysis

Let us study the stability of the basic state described in Equation (11) by employing small-amplitude disturbances in the form of normal modes, namely

$$P_i = P_{ib} + \epsilon f_i(x) e^{i(k_y y + k_z z - \omega t)}, \quad T_i = T_{ib} + \epsilon h_i(x) e^{i(k_y y + k_z z - \omega t)}, \quad i = 1, 2, \quad (13)$$

where  $\epsilon \ll 1$ ,  $\mathbf{k} = (0, k_y, k_z)$  is the wave vector, and  $\omega = \omega_R + i \omega_I$  is a complex parameter with  $\omega_R$  the angular frequency and  $\omega_I$  the temporal growth rate. By substituting Equation (13) into Equation (12) and linearising, one obtains

$$\begin{aligned} f_1'' - k^2 f_1 - ikS h_1 &= 0, \\ h_1'' - \left[ k^2 - i\omega + ikS \left( x - \frac{3}{4} \right) \right] h_1 + f_1' &= 0, \\ f_2'' - k^2 f_2 - ikS h_2 &= 0, \\ h_2'' - k^2 h_2 &= 0, \\ x = 0 : \quad f_1 &= 0, \quad h_1 = 0, \\ x = 1 : \quad f_1 &= f_2, \quad f_1' = \zeta f_2', \quad h_1 = h_2, \quad h_2' = 0, \\ x = 2 : \quad f_2' &= 0, \quad h_2 = 0, \end{aligned} \quad (14)$$

where a rescaled Rayleigh number  $S$  has been employed, namely

$$k S = k_z R. \quad (15)$$

With the definition (15),  $S$  turns out to be the dimensionless parameter governing the possible transition to instability for a given  $k$ . Since  $k_z \leq k$ , with the equality holding true for the transverse rolls ( $k_y = 0$ ), then the transverse rolls emerge as the perturbation modes liable to trigger the instability in every case at the lowest values of  $R$ . Hence, the transverse rolls are the most unstable modes. From Equation (14) one can readily find that

$$h_2 = 0, \quad f_2 = C_1 \cosh[k(2 - x)], \quad (16)$$

where  $C_1$  is an integration constant. By substituting the solution for  $f_2$  in the interface conditions reported in Equation (14) one obtains

$$f_1(1) = C_1 \cosh(k), \quad f_1'(1) = -C_1 \zeta k \sinh(k). \tag{17}$$

By eliminating  $C_1$ , an interface condition expressed only in terms of  $f_1$  is obtained, namely

$$f_1'(1) = -f_1(1) \zeta k \tanh(k). \tag{18}$$

For the limiting case  $\gamma \rightarrow \infty$ , the stability problem simplifies to the study of the fields inside layer 1, namely

$$\begin{aligned} f_1'' - k^2 f_1 - ikS h_1 &= 0, \\ h_1'' - \left[ k^2 - i\omega + ikS \left( x - \frac{3}{4} \right) \right] h_1 + f_1' &= 0, \\ x = 0 : \quad f_1 &= 0, \quad h_1 = 0, \\ x = 1 : \quad f_1' &= -f_1(1) \zeta k \tanh(k), \quad h_1 = 0. \end{aligned} \tag{19}$$

### 6. Results

The stability eigenvalue problem given by Equation (19) is here solved as a boundary value problem formulated as

$$\begin{aligned} f_1'' - k^2 f_1 - ikS h_1 &= 0, \\ h_1'' - \left[ k^2 - i\omega + ikS \left( x - \frac{3}{4} \right) \right] h_1 + f_1' &= 0, \\ f_1(0) = 0, \quad f_1'(0) = 1, \quad h_1(0) = 0, \quad h_1(1) = 0, \end{aligned} \tag{20}$$

where at  $x = 0$  we applied the scale fixing condition

$$f_1'(0) = 1, \tag{21}$$

allowing to break the scale invariance of the solution of the otherwise homogeneous problem (19). The boundary condition left

$$f_1'(1) = -f_1(1) \zeta k \tanh(k), \tag{22}$$

which is employed as a target for the root finding procedure which allows us to evaluate the pair  $(\omega, S)$  for fixed values of  $k$  and  $\zeta$ . The numerical technique employed for the solution of the stability eigenvalue problem is the shooting method. Details on the features of such method and its accuracy can be found in the literature [17,18]. In particular, Barletta [18] provided also a detailed description of the coding of such method by employing *Octave* [19].

The calculations are performed by utilizing the *Mathematica* software environment [20] and, in particular, the embedded functions `NDSolve` and `FindRoot`. The function `NDSolve` is used to find numerically the solution of the system of ordinary differential equations given by Equation (20). The function `FindRoot` is adopted to determine the eigenvalue pair  $(S, \omega)$  for prescribed input data  $(k, \zeta)$ .

The neutral stability curves are reported in Figure 3 where each curve is drawn for fixed values of the parameter  $\zeta$ . The latter parameter turns out to be a destabilizing parameter since the curves move downward as  $\zeta$  increases.

The local minima of  $S$  along the curves reported in Figure 3 are, by definition, the critical values for the onset of the thermal instability. These values,  $S_c$  and  $\omega_{R,c}$ , are displayed in Figure 4. This figure confirms the destabilizing role of the parameter  $\zeta$  just highlighted in the comment on Figure 3. One can note that the frame is cut for a particular value of  $S_c$  and  $\omega_{R,c}$ . This choice is due to the fact that  $\zeta$  has a lower threshold,  $\zeta_{min} = 2.57159$ , below which no neutral stability curve is present and, hence, no linear instability is possible. For this limiting value, we obtain



$$S_{c,max}(\xi_{min}) = 367.616, \quad \omega_{R,c,min}(\xi_{min}) = -40.3930. \tag{23}$$

It is worth noting that  $\xi_{min}$  identifies a minimum value of the curve  $\xi = \xi(S)$  and does not represent an asymptotic limit. Values of  $\xi > \xi_{min}$  yield more than one value of  $S$ : the critical one shown in Figure 4 and another value  $S > 367.616$ , relative to branches of the solution that are not relevant for the present linear stability analysis. Since Figure 4 reveals that the critical values of the angular frequency are always negative, one can conclude that the convective cells emerging at the onset of the instability drift downwards.

An interesting aspect to report is the distribution of isolines of streamfunction and temperature for the perturbed fields at a critical condition. From the definition of streamfunction

$$u = \frac{\partial \psi}{\partial z}, \quad w = -\frac{\partial \psi}{\partial x}, \tag{24}$$

and from Equation (1) one can relate the streamfunction to the fields  $f_1$  and  $f_2$  [15]

$$\psi_1 = -\frac{1}{ik} f'_1, \quad \psi_2 = -\frac{\xi}{ik} f'_2. \tag{25}$$

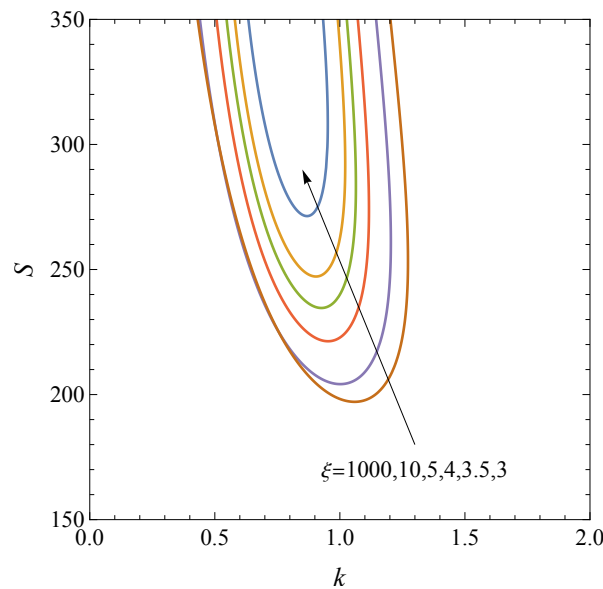


Figure 3. Neutral stability curves for fixed values of  $\xi$ .

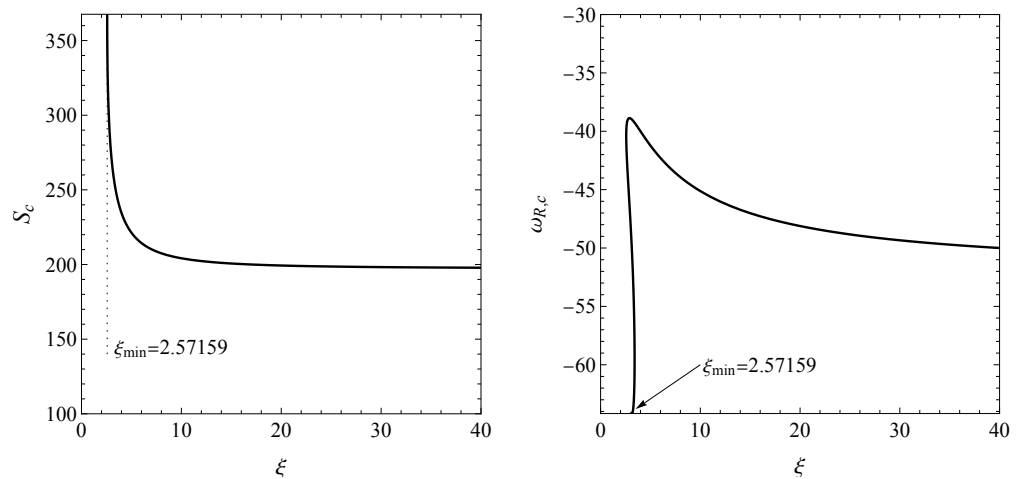
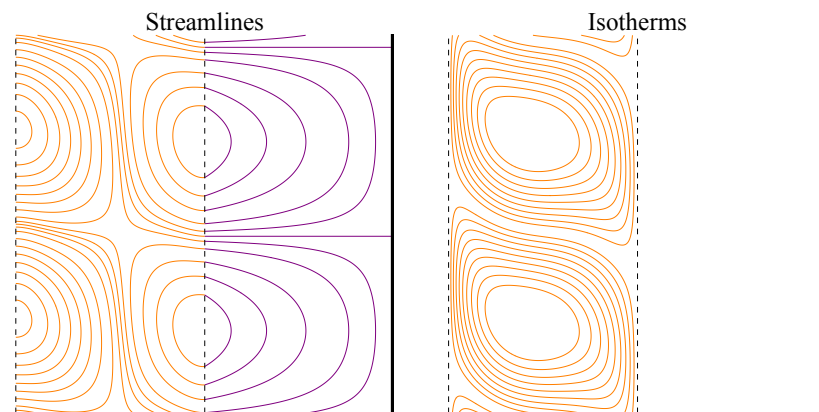


Figure 4. Critical values  $S_c$ , left-hand frame, and  $\omega_{R,c}$ , right-hand frame, versus  $\xi$ .



By employing Equation (14) together with Equation (25), in Figure 5, we obtain the isolines of streamfunction and temperature for  $\zeta = 5$ . One can note that the isotherms of the layer 2 are absent. This behaviour is a consequence of the assumption  $\gamma \rightarrow \infty$ , i.e., a thermal conductivity of layer 2 much greater than that of layer 1, which allowed us to infer that  $h_2 = 0$ . Since the increment in the value of  $\psi$  between neighboring isolines is a constant, it is also worth noting that the secondary cellular flow field in layer 1 is more intense than that in layer 2, which is due to the higher permeability of layer 2, being  $\zeta = 5$ .



**Figure 5.** Isolines of streamfunction and temperature for critical condition at  $\zeta = 5$ .

## 7. Conclusions

The possibility that an inhomogeneous vertical porous slab displays the emergence of a convective instability has been studied. This study is in the wake of other investigations regarding either continuously variable thermophysical properties in the horizontal direction or multilayer structures. In fact, previous studies have emphasised that suitable combinations of boundary conditions and heterogeneity of the porous material can trigger or prevent the onset of the convective cellular patterns inside the slab.

The influence of an open boundary together with the assumption of a slab made of two different porous layers is studied. The slab is characterised by two isothermal vertical boundaries at different temperatures: one boundary is open while the other is impermeable. The limiting case of a porous layer much more conductive than the other is investigated. The ratio  $\zeta$  between the permeabilities of the two layers turns out to be a key parameter, together with the choice of the temperature and velocity boundary conditions. After an analytical determination of the basic flow state, the linear stability analysis has been carried out numerically by employing the shooting method for differential eigenvalue problems.

The main conclusions are listed below:

- The inhomogeneous porous slab may undergo the onset of convective instability for a sufficiently large modified Darcy–Rayleigh number,  $S$ ; this result confirms that the considered horizontal asymmetry in the geometrical and physical configuration, with respect to the original problem solved by Gill [1], yields a possibly unstable basic state;
- An increase in the permeability ratio  $\zeta$  has a destabilising effect; indeed, the critical value of the Darcy–Rayleigh number  $S_c$  is a decreasing function of  $\zeta$ ;
- There is a minimum value of  $\zeta$ , given by  $\zeta_{min} = 2.57159$ , beyond which no instability arises; it is worth noting that this value does not correspond to an asymptotic behavior, but it identifies a minimum value for the curve  $\zeta = \zeta(S_c)$ ;
- The perturbation flow field tends to be more intense in the layer characterized by a lower thermal conductivity and permeability.

To the best of the authors' knowledge, there are not yet studies available in the literature showing all the possible combinations of heterogeneity and prescribed boundary conditions that may trigger or prevent the emergence of convection cells in a vertical porous

slab. A general formulation of a criterion for the existence of the instability can definitely be an important opportunity for a future development of this study.

**Author Contributions:** Conceptualization, S.L., M.C., A.B. and P.V.B.; methodology, S.L., M.C., A.B. and P.V.B.; software, S.L. and M.C.; validation, A.B. and P.V.B.; formal analysis, S.L., M.C., A.B. and P.V.B.; investigation, S.L., M.C., A.B. and P.V.B.; writing—original draft preparation, S.L., M.C., A.B. and P.V.B.; writing—review and editing, S.L., M.C., A.B. and P.V.B.; supervision, A.B.; project administration, A.B.; funding acquisition, A.B. All authors have read and agreed to the published version of the manuscript.

**Funding:** This research was funded by Italian Ministry of Education and Scientific Research grant number PRIN 2017F7KZWS.

**Data Availability Statement:** Data sharing is not applicable to this article.

**Conflicts of Interest:** The authors declare no conflict of interest. The funders had no role in the design of the study; in the collection, analyses, or interpretation of data; in the writing of the manuscript, or in the decision to publish the results.

## References

1. Gill, A.E. A proof that convection in a porous vertical slab is stable. *J. Fluid Mech.* **1969**, *35*, 545–547. [[CrossRef](#)]
2. Rees, D.A.S. The stability of Prandtl-Darcy convection in a vertical porous layer. *Int. J. Heat Mass Transf.* **1988**, *31*, 1529–1534. [[CrossRef](#)]
3. Straughan, B. A nonlinear analysis of convection in a porous vertical slab. *Geophys. Astrophys. Fluid Dyn.* **1988**, *42*, 269–275. [[CrossRef](#)]
4. Lewis, S.; Bassom, A.P.; Rees, D.A.S. The stability of vertical thermal boundary-layer flow in a porous medium. *Eur. J. Mech. B Fluids* **1995**, *14*, 395–407.
5. Rees, D.A.S.; Lage, J.L. The effect of thermal stratification on natural convection in a vertical porous insulation layer. *Int. J. Heat Mass Transf.* **1996**, *40*, 111–121. [[CrossRef](#)]
6. Rees, D.A.S. The Effect of Local Thermal Nonequilibrium on the Stability of Convection in a Vertical Porous Channel. *Transp. Porous Media* **2011**, *87*, 459–464. [[CrossRef](#)]
7. Scott, N.L.; Straughan, B. A Nonlinear Stability Analysis of Convection in a Porous Vertical Channel Including Local Thermal Nonequilibrium. *J. Math. Fluid Mech.* **2013**, *15*, 171–178. [[CrossRef](#)]
8. Barletta, A. A proof that convection in a porous vertical slab may be unstable. *J. Fluid Mech.* **2015**, *770*, 273–288. [[CrossRef](#)]
9. Celli, M.; Barletta, A.; Rees, D.A.S. Local thermal non-equilibrium analysis of the instability in a vertical porous slab with permeable sidewalls. *Transp. Porous Media* **2017**, *119*, 539–553. [[CrossRef](#)]
10. Barletta, A.; Celli, M.; Ouarzazi, M.N. Unstable buoyant flow in a vertical porous layer with convective boundary conditions. *Int. J. Therm. Sci.* **2017**, *120*, 427–436. [[CrossRef](#)]
11. Barletta, A.; Rees, D.A.S. On the onset of convection in a highly permeable vertical porous layer with open boundaries. *Phys. Fluids* **2019**, *31*, 074106. [[CrossRef](#)]
12. Barletta, A.; Celli, M. Anisotropy and the onset of the thermoconvective instability in a vertical porous layer. *J. Heat Transf.* **2021**, *143*, 102601. [[CrossRef](#)]
13. Zhao, C.; Opolot, M.; Liu, M.; Bruno, F.; Mancin, S.; Flewell-Smith, R.; Hooman, K. Simulations of melting performance enhancement for a PCM embedded in metal periodic structures. *Int. J. Heat Mass Transf.* **2021**, *168*, 120853. [[CrossRef](#)]
14. Imbabi, M.S.E. Modular breathing panels for energy efficient, healthy building construction. *Renew. Energy* **2006**, *31*, 729–738. [[CrossRef](#)]
15. Barletta, A.; Celli, M.; Lazzari, S.; Brandão, P.V. Gill’s problem in a sandwiched porous slab. *J. Fluid Mech.* **2022**, *952*, A32. [[CrossRef](#)]
16. Shankar, B.M.; Shivakumara, I.S. Gill’s stability problem may be unstable with horizontal heterogeneity in permeability. *J. Fluid Mech.* **2022**, *943*, A20. [[CrossRef](#)]
17. Straughan, B. *Stability and Wave Motion in Porous Media*; Springer: New York, NY, USA, 2008.
18. Barletta, A. *Routes to Absolute Instability in Porous Media*; Springer: New York, NY, USA, 2019.
19. Eaton, J.W.; Bateman, D.; Hauberg, S.; Wehbring, R. *Gnu Octave*; The Octave Project Developers, 2023. Available online: <https://octave.org/> (accessed on 1 June 2023).
20. Wolfram, S. *The Mathematica Book, Fifth Edition*; Wolfram Media, Wolfram Research Inc.: Champaign, IL, USA, 2003.

**Disclaimer/Publisher’s Note:** The statements, opinions and data contained in all publications are solely those of the individual author(s) and contributor(s) and not of MDPI and/or the editor(s). MDPI and/or the editor(s) disclaim responsibility for any injury to people or property resulting from any ideas, methods, instructions or products referred to in the content.